Solar-Terrestrial Physics. 2026, vol. 12, iss. 1, pp. 40–49. DOI: 10.12737/stp-121202606. © 2026 K.G. Ratovsky, I.V. Medvedeva. Published by INFRA-M Academic Publishing House

DOI: 10.12737/stp-121202606
EDN: OXHPVR

Received August 28, 2025
Accepted November 25, 2025

COMPARATIVE ANALYSIS OF RESPONSES OF MINIMUM FREQUENCY OF IONOGRAM REFLECTIONS AND MESOSPHERE-LOWER THERMOSPHERE TEMPERATURE TO WINTER SUDDEN STRATOSPHERIC WARMINGS

K.G. Ratovsky
Institute of Solar-Terrestrial Physics SB RAS, Irkutsk, Russia, ratovsky@iszf.irk.ru

I.V. Medvedeva
Institute of Solar-Terrestrial Physics SB RAS, Irkutsk, Russia, ivmed@iszf.irk.ru
Obukhov Institute of Atmospheric Physics RAS, Moscow, Russia

Abstract. The paper is devoted to the comparative analysis of the responses of the minimum frequency of reflections on ionograms (f_{min}) and the mesosphere-low thermosphere (MLT) temperature to the sudden stratospheric warmings (SSWs) in 2008, 2009, and 2013. The experimental basis for the research is the f_{min} measurements with the DPS-4 digital ionosonde in Irkutsk, the Aura/MLS satellite data on the atmospheric temperature at different altitudes, and the data on the rotational temperature of the hydroxyl molecule obtained from spectrometric measurements at ~100 km from Irkutsk. Comparative analysis of the behavior of f_{min} and the MLT temperature has revealed both a case of high correlation (SSW 2008) and no correlation (SSW 2009), along with an intermediate variant during the SSW 2013. The paper discusses the reasons for the different correlations between the analyzed parameters.

Keywords: minimum frequency of ionogram reflections, temperature, mesosphere-low thermosphere, MLT, sudden stratospheric warming, correlation analysis.

INTRODUCTION

One of the most important problems of physics of near-Earth space is to study the response of the upper neutral atmosphere and ionosphere to extreme events in underlying atmospheric layers. The most significant meteorological disturbances, covering large spatial and time scales and leading to violations of the thermodynamic regime in a large range of atmospheric heights, include winter sudden stratospheric warmings (SSWs). Currently, one of the main hypotheses for the occurrence of stratospheric warmings is considered to be the wave theory in which the prevailing mechanism for the development of stratospheric warmings is planetary-scale wave disturbances [Matsuno, 1971]. The mechanism consists in amplifying planetary waves propagating upward from the troposphere and their interaction with the mean wind flow. This interaction leads to a weakening or reversal of the western winter stratospheric flow. SSW events are the most striking example of the interconnection between various atmospheric layers. SSW effects can be observed in a wide range of latitudes, from the pole to the tropics, and disturbances cover a wide height range, from the troposphere to the thermosphere [Vargin, Medvedeva, 2015; Yigit, Medvedev, 2015]. By now it has been established that major SSW events have a noticeable effect on the upper atmosphere. Even Shefov [1973] drew attention to the noticeable cooling of the mesosphere – lower thermosphere (MLT) during SSWs and subsequent temperature variations. Yigit and Medvedev [2015] have shown that disturbances in the lower and middle atmosphere during SSWs cause significant anomalies in the thermosphere and ionosphere. Effects of winter SSWs on MLT has been revealed from measurements of the OH rotational temperature [Walterscheid et al., 2000; Shepherd et al., 2010; Perminov, Pertsev, 2013; Medvedeva, Ratovsky, 2018], measurements with meteor radars and lidars [Hoffmann et al., 2002, 2007], and satellite data [Siskind et al., 2005; Manney et al., 2009]. During SSWs, activity of waves of different time scales increases [Limpasuvan et al., 2012; Yigit, Medvedev, 2015]. Experimental and theoretical investigations into ionospheric plasma parameters have made it possible to detect SSW-driven effects at ionospheric heights of the F layer almost throughout the latitude range of the winter hemisphere [Pancheva, Mukhtarov, 2011; Klimenko et al., 2013; Goncharenko et al., 2013; Polyakova et al., 2014; Shpynev et al., 2015; Lukianova et al., 2015; Medvedeva, Ratovsky, 2018; Yasyukevich, 2018, Yasyukevich et al., 2022]. A number of studies have indicated that SSW effects on conditions in the upper neutral atmosphere and ionosphere depend on the region of observation. For example, the presence of longitude differences in the SSW effects on MLT was shown in [Medvedeva et al., 2019] according to observations of OH emission at the stations Tory and Zvenigorod. The calculations carried out in that work with MUAM (the middle and upper atmosphere model) suggest that the detected longitude differences in the SSW effect are due to longitude differences in the behavior of the predominant vertical wind at the OH emission height for the analyzed event. Shpynev et al. [2015], using radio sounding data from Russian ionosondes during SSWs in

2009 and 2013, have indicated that the ionospheric response to SSW depends on the location of an ionosonde relative to the stratospheric circulation pattern.

Despite the large number of works dealing with the ionospheric response to SSW, the vast majority of them contain results of research into the effects at the ionospheric F-layer heights. Previously, we have examined SSW effects of different types occurring at the mesopause and in the F2-region in February–March 2016, February 2017, February 2018, and January 2019 from spectrometric and radiophysical observations in Eastern Siberia. We analyzed data on the rotational temperature of the hydroxyl molecule and on the F2-layer peak electron density N_mF2, using the existing method of estimating atmospheric and ionospheric variability, which allows us to study manifestations of wave activity in a wide range of heights of the upper atmosphere [Medvedeva, Ratovsky, 2015]. It was found that during all the events considered increased manifestations of atmospheric wave activity were observed at the MLT and F2-region heights, yet the nature of these manifestations was different [Medvedeva, Ratovsky, 2018, 2020].

Unlike our previous works, where SSW effects were examined at F-layer heights, in this research we have selected a characteristic related to the lower ionosphere — the minimum frequency of reflections f_{min}, i.e. the lowest frequency at which traces of reflections from the ionosphere are observed in a vertical sounding ionogram. According to the well-known monograph [Davies, 1973], the differential non-deviative absorption of short radio waves in the ionosphere is proportional to the product of the electron density N_e by the collision frequency ν of electrons with neutral particles (neutrals for short) and inversely proportional to the squared frequency of a radio signal f. The total absorption is determined by the height integral of the product $N_e \cdot \nu$, with the main contribution to the integral being made by the D layer (~70–90 km) or the lower part of the E layer (~90–95 km). Due to the fact that absorption is inversely proportional to f^2, f_{min} sets a critical level of absorption at which the signal-to-noise ratio is sufficient to observe reflections from the ionosphere (at $f<f_{min}$, absorption exceeds the critical level and there are no reflections from the ionosphere). Thus, f_{min} increases/decreases with increasing/decreasing N_e and ν in the D layer and the lower part of the E layer.

There are a number of experimental works dealing with the study of the effect of atmospheric disturbances on absorption of radio waves of various ranges. Pancheva et al. [1991] detected both short-period (5–7 days) and long-period (10.5–13.0 days) fluctuations in absorption of short radio waves in the lower ionosphere in winter, with short-period fluctuations attributed to an increase in activity of stationary planetary waves with zonal wave number 2 (SPW2); and long-period fluctuations, to an increase in activity of stationary planetary waves with zonal wave number 1 (SPW1). Schmitter [2011] found a correlation of amplitudes of VLF and LF signals and f_{min}, which characterizes absorption in the HF band, with activity of planetary waves (mainly with ~16-day periods). Schneider et al [2025] have revealed that during three of the four SSW events under study there is an increase in the amplitude of VLF signals during SSW and a decrease in the amplitude of VLF signals during rises of the stratopause height.

The mechanisms of the effect of atmospheric disturbances on the electron density and the electron-neutral collision frequency in the D layer have been examined in a number of works [Kazimirovsky et al., 2003; Siskind et al., 2017; Schneider et al., 2025; Schmitter, 2011]. Kazimirovsky et al. [2003] note the following atmospheric factors that increase the electron density in the D layer: a) an increase in the mesopause temperature impeding the formation of cluster ions; b) the downward transport of nitric oxide NO; c) a drop in pressure near the mesopause, reducing the optical thickness for solar UV radiation and thereby increasing the rate of ionization. Siskind et al. [2017] through numerical simulation show that the NO concentration makes a significant contribution to absorption of short radio waves at midlatitudes. Maximum differential absorption at a frequency of 5 MHz is intrinsic to the lower part of the E layer (~95 km). Schneider et al. [2025] propose the combined mechanism of the effect of atmospheric disturbances to explain absorption variations during SSWs. The electron density in the D layer decreases with increasing recombination rate due to a decrease in the mesospheric temperature and an increase in the water vapor content. The electron-neutral collision frequency decreases with decreasing mesospheric temperature. Both effects lead to a decrease in absorption of VLF signals. Schmitter [2011], using modeling and temperature data from the SABER satellite, show that the periods of pressure rise and fall in the mesosphere coincide with periods of increased and decreased absorption of VLF/LF signals respectively. This coincidence is explained by the proportionality of the electron-neutral collision frequency to the pressure in the mesosphere.

The above-mentioned mechanisms allow us to expect a correlation between f_{min} and mesospheric temperature variations. A temperature rise leads to an increase in both N_e [Kazimirovsky et al., 2003; Schneider et al., 2025] and ν [Schneider et al., 2025; Schmitter, 2011], which increases absorption and f_{min}. A temperature drop leads to the opposite effect. The aforementioned correlation may be disrupted due to the effects of other factors: a change in the chemical composition [Kazimirovsky et al., 2003; Siskind et al., 2017; Schneider et al., 2025] or the effects of solar flares and geomagnetic disturbances. Additional factors that break the correlation will be discussed below.

The purpose of this study is to comparatively analyze the responses of f_{min} and MLT temperature to SSWs in 2008, 2009, and 2013. The comparative analysis method and the data in use are described in detail in section “Data Analysis Method”.

DATA ANALYSIS METHOD

The study is based on experimental data from the complex of instruments of the Institute of Solar-Terrestrial Physics SB RAS (ISTP SB RAS) and Aura MLS satellite data [http://disc.gsfc.nasa.gov/Aura]. The ISTP SB RAS data includes the minimum frequency of

ionogram reflections f_{min} obtained by the DPS-4 digital vertical sounding ionosonde in Irkutsk (52.3° N, 104.3° E) and the rotational temperature of the hydroxyl molecule (OH(6-2) band, 834.0 nm, ~87 km) derived from spectrometric measurements at the ISTP SB RAS Geophysical Observatory (51.8° N, 103.1° E, Tory village). Satellite data represents vertical atmospheric temperature profiles obtained when the satellite passed over the analyzed region during the daytime. We have also used MERRA-2 reanalysis data on the temperature and dynamics of the middle atmosphere of the Northern Hemisphere [http://gmao.gsfc.nasa.gov/research/merra/].

The rotational temperature of the hydroxyl molecule reflects the atmospheric temperature at the mesopause. Data on the rotational temperature of the OH molecule was analyzed only for the SSW 2013, since no regular spectrometric observations of hydroxyl emission were made during the earlier events considered. For the analysis, we calculated the residual variations in OH temperature after removal of regular seasonal variations. Seasonal variations were determined by the least square approximation of the obtained series of temperature values averaged over the night by a function of the form

$$T = \bar{T} + \sum_{n=1}^{3} A_n \cos\left(\frac{2\pi n}{365.25}\left(t_d - \varphi_n\right)\right),$$

where $\bar{T}$ is the average temperature; n is the harmonic number; A_n and φ_n are its amplitude and phase; t_d is the day of the year. The approximation was carried out by the first three harmonics of seasonal variations with periods of 12, 6, and 4 months.

The paper examines day-to-day variations in daytime average (9–15 LT) f_{min}, as well as disturbances of Δf_{min}, which represent the relative difference between the observed values $f_{min\ obs}$ and the values of the moving 27-day median $f_{min\ med}$:

$$\Delta f_{min}\,(\%) = 100\,\%\left(f_{min\ obs} - f_{min\ med}\right) / f_{min\ med}.$$

The calculated Δf_{min} disturbances are compared with residual OH temperature variations.

To investigate the relationship between f_{min} and the atmospheric temperature T, we have conducted a correlation analysis of day-to-day variations in f_{min} and T at different heights.

COMPARATIVE ANALYSIS OF RESPONSES OF MINIMUM FREQUENCY OF IONOGRAM REFLECTIONS AND TEMPERATURE OF THE MESOPAUSE REGION

For the research, we have selected SSWs occurring in January–February 2008, January 2009, and January 2013. Figure 1 illustrates variations in the zonal characteristics of the stratosphere at an altitude of 10 hPa (~32 km) according to MERRA-2 reanalysis data: the mean zonal (60° N) wind (top panels) and the mean zonal (60–90° N) temperature (bottom panels) for the analyzed events.

Analysis of zonal characteristics of the middle atmosphere over the Northern Hemisphere from MERRA-2 reanalysis data has shown the following. In January–February 2008, four SSWs occurred in the Northern Hemisphere, the last of which was accompanied by the change of the mean zonal wind direction at 60° N and 10 hPa from westerly to easterly on February 22–28, 2008 and can be classified as major SSW (see Figure 1, *a*). Mean zonal temperature maxima for the SSW 2008 were observed on January 25, February 06, 17, and 24. Major SSW in January 2009 was the strongest on record, since mid-January there was a sharp increase in the mean zonal (60–90° N) temperature by more than 50 K, the maximum value of 253 K was recorded on January 23. The mean zonal wind changed direction on January 25 – February 22, 2009 (see Figure 1, *b*). The third SSW occurring in January 2013 is also classified as major. Since the end of December 2012, the mean zonal temperature increased by ~35 K, with a maximum value of 235 K detected on January 12. The mean zonal wind changed direction on January 06–28, 2013 (see Figure 1, *c*).

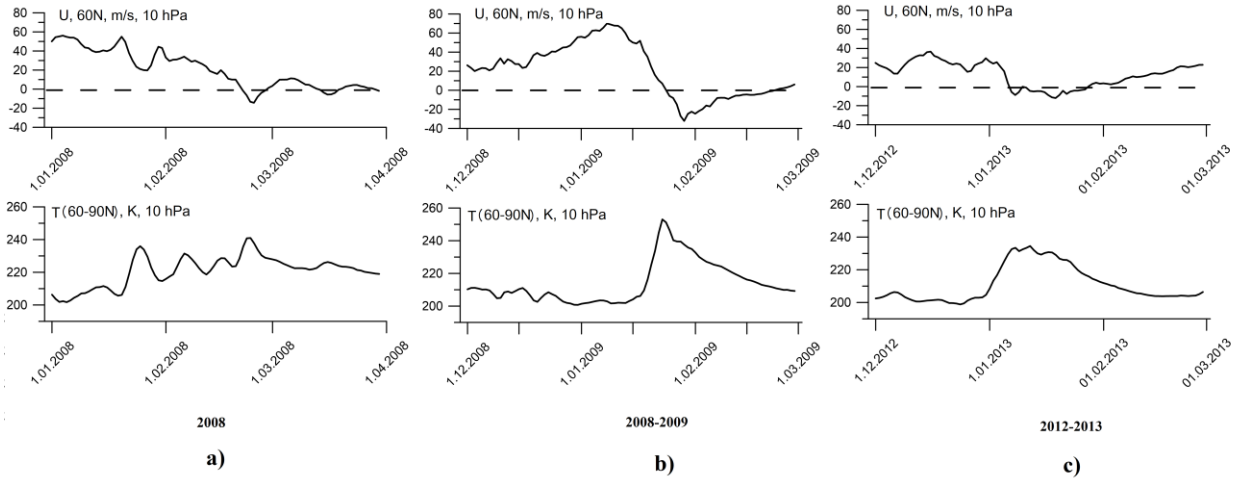

Figure 1. Zonal characteristics of the stratosphere at an altitude of 10 hPa (~32 km) according to MERRA-2 reanalysis data for January 01 –April 01, 2008 (*a*), December 01, 2008 – March 01, 2009 (*b*), and December 01, 2012 – March 01, 2013 (*c*): top panels — mean zonal (60° N) wind; bottom panels — mean zonal (60–90° N) temperature

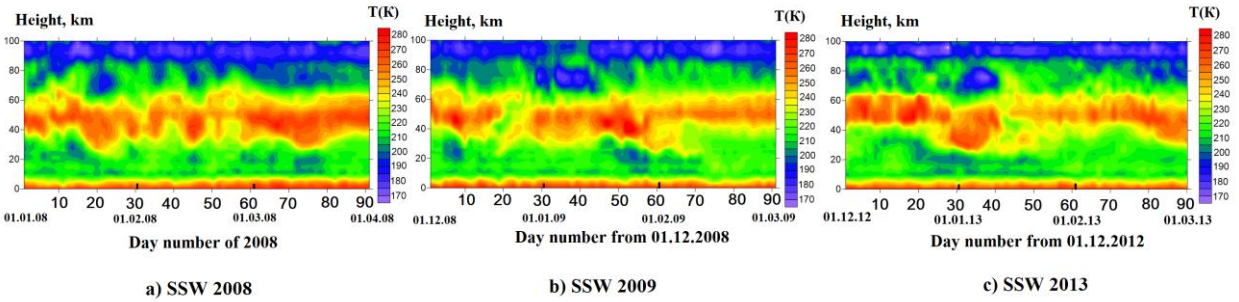

Figure 2. Vertical profiles of atmospheric temperature according to data from daytime passages of the Aura/MLS satellite in the analyzed region for January 01 – April 01, 2008 (*a*), December 01, 2008 – March 01, 2009 (*b*), and December 01, 2012 – March 01, 2013 (*c*)

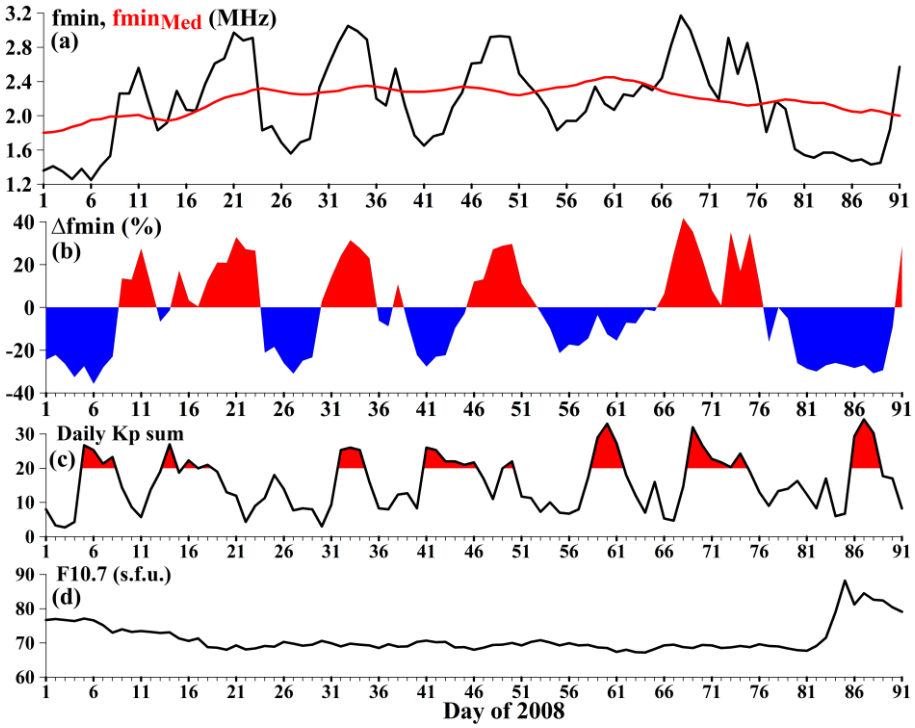

Figure 3. Day-to-day variations of analyzed parameters for January 01 — March 31, 2008 (days 01–91 in 2008): *a* — f_{min} (black curve) and $f_{min\ med}$ (red curve); *b* — Δf_{min} (%); *c* — the daily K_p sum (red color highlights disturbed conditions); *d* — the $F10.7$ index

The Aura/MLS data acquired over the region in question during the daytime was used to analyze the atmospheric temperature over Irkutsk. Figure 2 displays vertical profiles of the atmospheric temperature for January 01 – April 01, 2008 (*a*), December 01, 2008 – March 01, 2009 (*b*), December 01, 2012 – March 01, 2013 (*c*). Analysis of satellite data revealed that significant temperature disturbances in the middle atmosphere were observed during all SSWs under study.

SUDDEN STRATOSPHERIC WARMING IN 2008

Figure 3, *a* shows day-to-day variations of daytime average f_{min} and $f_{min\ med}$ for January 01 – March 31, 2008 (days 01–91 in 2008). Panels *b*, *c*, and *d* in Figure 3 depict day-to-day variations of the relative disturbance Δf_{min} [%], the daily K_p sum index of geomagnetic activity, and the solar activity index $F10.7$ for the same period. The daily K_p sum is the sum of eight K_p indices for a given day. Throughout the analyzed interval (01–91), $F10.7$ varies from 67 to 88 with an average value of 71; and on the interval 10–83, from 67 to 73 with an average value of 69. Thus, for most analyzed interval the behavior of $F10.7$ corresponds to solar minimum (low values with minor variations) with a slight increase in the index at the beginning and end of the interval.

On the entire analyzed interval (01–91), the daily K_p sum varies from 2.7 to 34.3 with an average value of 15.8. For 60 of 91 days, the daily K_p sum does not exceed 20, which corresponds to quiet geomagnetic conditions; for 31 of 91 days, K_p is typical for disturbed conditions. The analyzed interval includes three weak geomagnetic storms: February 29 – March 01 (days 60–61), K_p=5+; March 09 (day 69), K_p=6–; March 26–27 (days 86–87), K_p=5o. Throughout the analyzed interval (01–91), f_{min} varies from 1.3 to 3.2 MHz with an average value of 2.2 MHz and a standard deviation of 0.5 MHz. Figure 3, *b* indicates that Δf_{min} disturbances are quasi-periodic fluctuations with periods (~17–20 days) and a

range approximately from –40 to +40 %. According to [Pancheva et al., 1991], such long-period intense fluctuations may be associated with increased SPW1 activity.

To examine the relationship of f_{min} with the atmospheric temperature T, we have performed a correlation analysis of day-to-day variations in f_{min} and T derived from Aura/MLS data at different MLT heights. The analysis has shown that the best correlation (the highest and positive) occurs for the atmospheric temperature at an altitude of 92 km (T92), which is consistent with the results of [Siskind et al., 2017], where through numerical simulation it has been revealed that maximum differential absorption at a frequency of 5 MHz corresponds to the lower part of the E layer (~95 km). Figure 4 illustrates day-to-day variations of daytime average f_{min} with superimposed variations of T92.

Initially, the correlation was calculated for January 25 – February 24, 2008 (days 25–55), which matches the period between the first (January 25) and the last maximum of the mean zonal temperature for the SSW 2008. For this interval, the correlation coefficient R was 0.80, with a two-day shift (January 27 – February 26, days 27–57), R increased to 0.89; and with an extension of the interval (January 17 – March 12, days 17–72), R decreased to 0.62. One of the factors explaining the decrease in the correlation during the extension of the interval to January 17 – March 12 (days 17–72) may be the geomagnetic storms on February 29 – March 01 (days 60–61) and March 09 (day 69). The high correlation coefficient between f_{min} and T92 suggests that atmospheric temperature variations are the dominant factor affecting f_{min} variations. The coefficient of determination R^2=0.79 means ~80 % temperature contribution to changes in f_{min} and hence in absorption of short radio waves.

SUDDEN STRATOSPHERIC WARMING IN 2009

Figure 5 shows day–to-day variations of the same parameters as in Figure 3, but for January 01 – April 01, 2009 (01–91 days in 2009). Throughout the analyzed interval (01–91), F10.7 varies from 66 to 71 with an average value of 68. Thus, on the entire analyzed interval the behavior of F10.7 corresponds to solar minimum (low values with minor variations).

Throughout the interval (01–91), the daily K_p sum varies from 0.3 to 24.7 with an average value of 8.5, which is ~1.9 times smaller than in 2008. Except for three days, the daily K_p sum does not exceed 20, which is peculiar to quiet geomagnetic conditions. The analyzed interval does not include any geomagnetic storms. Thus, geomagnetic activity was much lower in 2009 than in 2008.

On the entire interval (01–91), f_{min} varies from 1.4 to 2.8 MHz with an average value of 1.8 MHz and a standard deviation of 0.22 MHz. On the interval 19–91, f_{min} varies from 1.4 to 2.2 MHz with an average value of 1.7 MHz and a standard deviation of 0.12 MHz. Thus, in 2009 f_{min} shows lower averages and standard deviations than in 2008. Unlike 2008, there are no quasi-periodic fluctuations in Δf_{min} disturbances; excepting four days, the fluctuation range does not exceed ±17 %.

A possible reason for the absence of intense quasi-periodic disturbances of Δf_{min} could be the absence of corresponding atmospheric temperature disturbances at 92 km. Figure 6 illustrates day-to-day variations of daytime average f_{min} with superimposed variations of T92 for 2009.

Unlike 2008, in 2009 there is a sharp decrease in T92 by 25 K from day 9 to 19. Later on, T92 variations in 2009 are quasi-periodic. The first wavetrain with ~8 K amplitude and ~9 day quasi-period is observed from day ~9 to 28. The next wavetrain with ~15 K amplitude and ~24 day quasi-period occurs from day ~28 to 52. The final two wavetrains with ~8 K amplitude and ~18 day quasi-period are recorded from day ~52 to 88. In contrast to 2008, in 2009 there is no correlation between f_{min} and T92 variations although the amplitudes of T92 variations are comparable in both cases.

Comparison between variations in f_{min} and temperatures at other MLT heights also did not reveal any correlation. Possible reasons for such different behavior of f_{min} during the SSWs 2008 and 2009 are discussed in section “Discussion and Interpretation of the Results”.

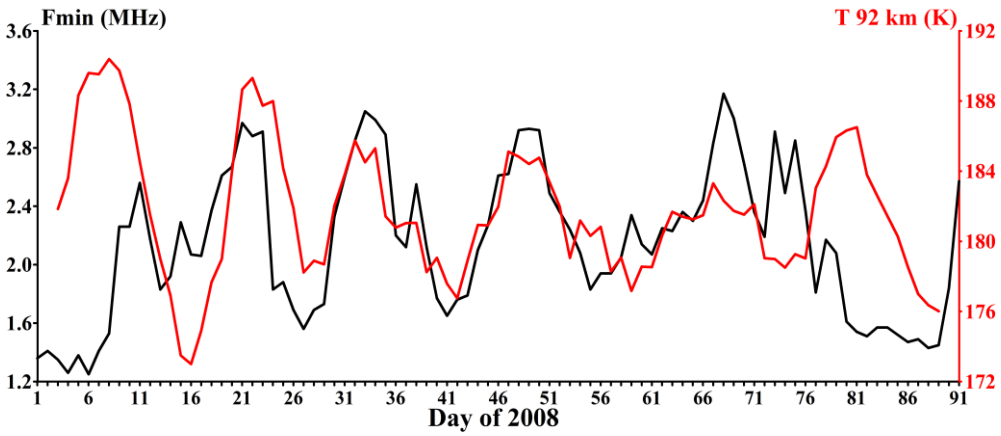

Figure 4. Day-to-day variations of daytime average f_{min} (black curve) with superimposed temperature variations at an altitude of 92 km (T92, red curve)

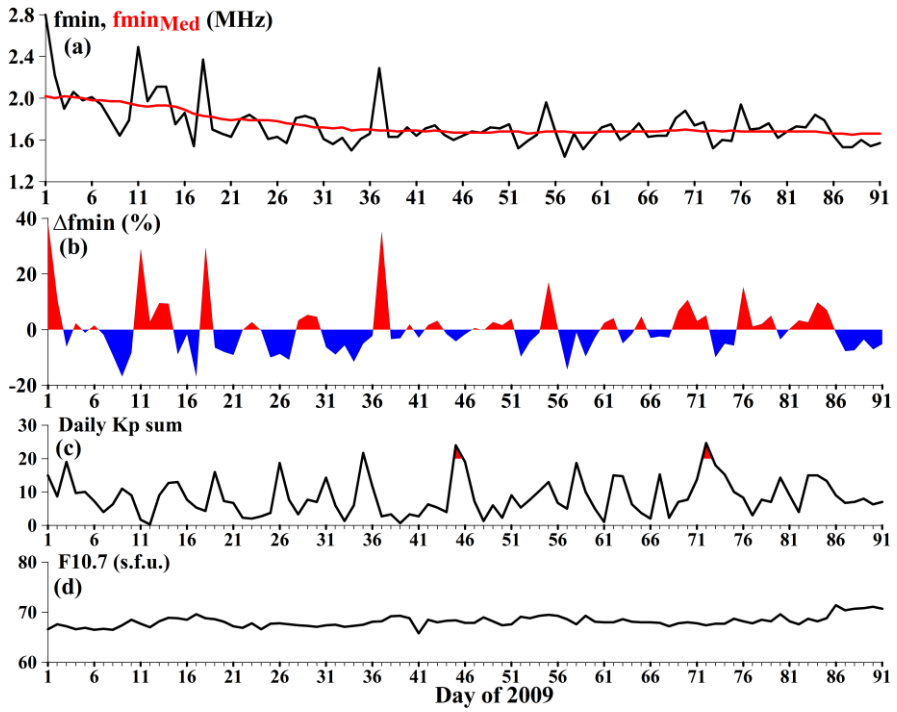

Figure 5. Day-to-day variations of the same parameters as in Figure 3, but for January 01 – April 01, 2009 (01–91 days in 2009)

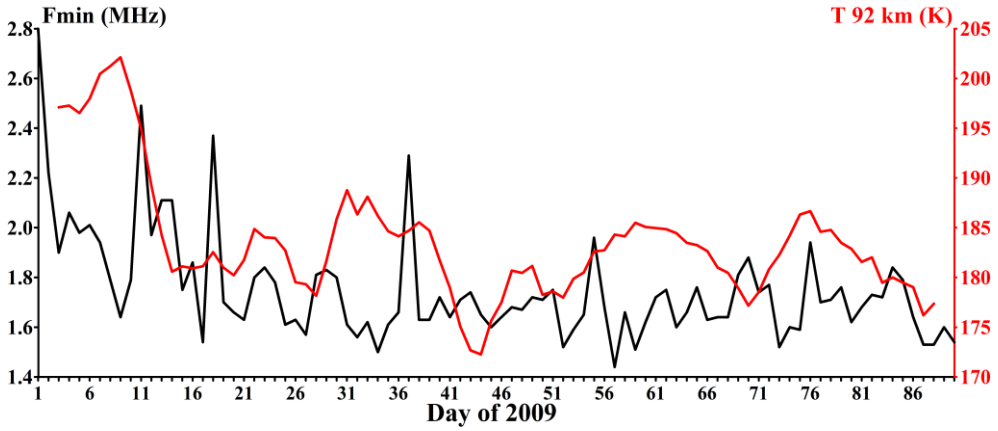

Figure 6. Day-to-day variations of daytime average f_{min} (black curve) with superimposed variations of $T92$ (red curve) for 2009

SUDDEN STRATOSPHERIC WARMING IN 2013

Figure 7 exhibits day-to-day variations of the same parameters as in Figure 3, but for December 01, 2012 – March 01, 2013 (days –30–60 in 2013). On the entire analyzed interval (–30–60), $F10.7$ varies from 93 to 168 with an average of 110. Unlike 2008 and 2009, in 2013 the behavior of $F10.7$ corresponds to moderate solar activity with a significant change in the analyzed interval (max/min ~1.8). The effect of the significant change in $F10.7$ on the correlation between T and f_{min} variations is analyzed in section "Discussion and Interpretation of the Results".

Throughout the interval (–30–60), the daily K_p sum varies from 0.7 to 35 with an average of 9.3. Except four days, the daily K_p sum does not exceed 20, which is peculiar to quiet geomagnetic conditions. The analyzed interval includes one weak geomagnetic storm: March 01 (day 60). Thus, in 2013 geomagnetic activity was much lower than in 2008 and slightly higher than in 2009.

Throughout the interval (–30–60), f_{min} varies from 1.7 to 3.6 MHz with an average of 2.3 MHz and a standard deviation of 0.4 MHz. Average f_{min} and the standard deviation of f_{min} are close to the values of 2008. On the interval 01–39 (January 01 – February 08), intense fluctuations with a range of ~–4 to +51 % are observed in Δf_{min} disturbances. Unlike 2008, the fluctuations are asymmetric (the positive amplitude is ~2 times higher than the negative one) and their recurrence is much less pronounced.

As for 2008, we have carried out a correlation analysis of day-to-day variations in f_{min} and T at different MLT heights. Similarly to the SSW 2008, the best correlation (the highest and positive) was found for $T92$. Figure 8 shows day-to-day variations of daytime average f_{min} with superimposed variations of $T92$ for 2013.

Initially, the interval January 06–28, 2013 (days 06–28) was chosen to calculate the correlation, which corre-

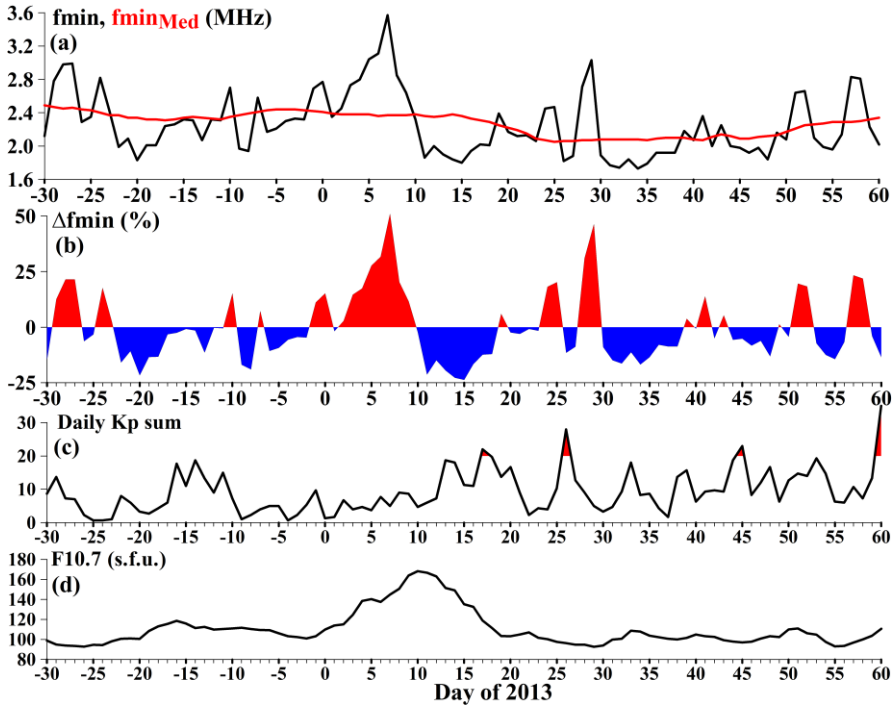

Figure 7. Day-to-day variations of the same parameters as in Figure 3, but for December 01, 2012 – March 01, 2013 (days –30–60 in 2013)

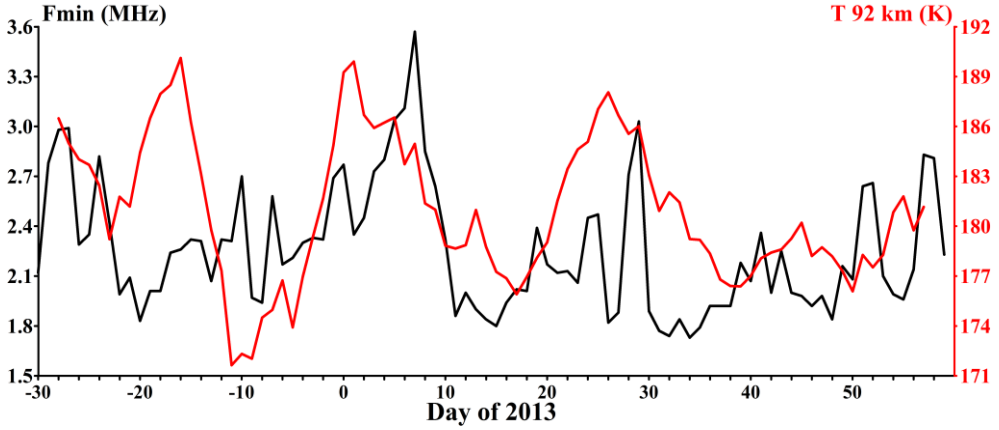

Figure 8. Day-to-day variations of daytime average f_{min} (black curve) with superimposed variations of $T92$ (red curve) for 2013

sponded to the interval of the mean zonal wind reversal for the SSW 2013. For this interval, the correlation coefficient R turned out to be low, 0.34; however, when the analysis interval was shifted three days back (January 03–25.01, days 03–25), R increased to 0.66. The coefficient of determination R^2=0.44 can be interpreted as a 44 % contribution of temperature to variations in f_{min} and hence in absorption of short radio waves.

Figure 9 illustrates variations in Δf_{min} disturbances and residual temperature variations in the mesopause region, obtained from OH emission measurements, for December 01, 2012 – March 01, 2013. Day-to-day temperature variations are mainly caused by the effect of planetary waves. It has been found that during major disturbances of the temperature and dynamics of the middle atmosphere and the mean zonal wind reversal during the SSW 2013 (see Figure 1, *c*) increased variability of Δf_{min} and ΔT was observed (see Figure 9), which may be due to intensification of planetary wave activity in the upper atmosphere during SSWs.

Thus, the correlation analysis of the day-to-day variations in f_{min} and T at an altitude of 92 km has revealed three different cases: high correlation for the SSW 2008, no correlation for the SSW 2009, and moderate correlation for the SSW 2013.

DISCUSSION AND INTERPRETATION OF THE RESULTS

In interpreting the results, the main problem is to explain the lack of correlation between the day-to-day variations in f_{min} and $T92$ for the SSW 2009. In Introduction, we have noted that the correlation may be disrupted by other factors such as solar flares and geomagnetic disturbances. Nonetheless, the SSW 2009 featured the lowest solar and geomagnetic activity compared to

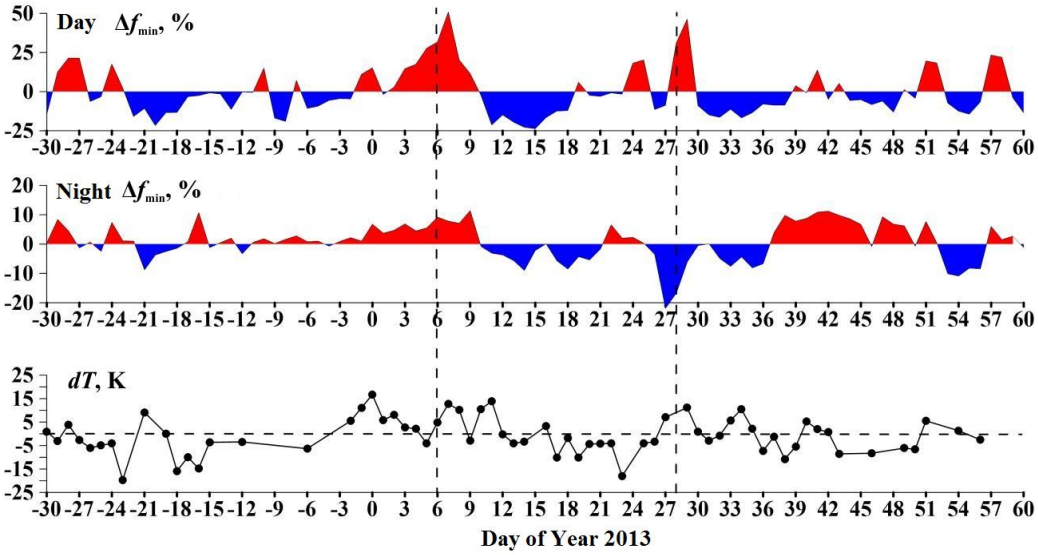

Figure 9. Variations in disturbances of daytime (top panel) and nighttime (middle panel) Δf_{min} and residual deviations of the mesopause temperature dT (bottom panel) after excluding seasonal variations for December 01, 2012– March 01, 2013. Vertical lines mark the dates of the zonal (60° N, 10 hPa) wind reversal

other SSWs, so the lack of correlation is not related to the above factors. In Introduction, we have mentioned that the total absorption is determined by the height integral of the product $N_e \cdot \nu$, and disruption of the correlation may be caused by anticorrelation between temperature variations at different heights. To verify this version, the correlation coefficients between temperature variations at heights of 92, 88, 84, and 80 km were calculated for all SSWs under study. The calculations showed that the correlation coefficients are always positive at adjacent heights (i.e., with a difference of 4 km) and vary from 0.35 to 0.92. The highest correlation coefficient between $T92$ and $T88$ was found for the SSW 2009 (0.92); slightly lower, for the SSW 2008 (0.73); and the lowest, for the SSW 2013 (0.53). Thus, the lack of correlation between the day-to-day variations in f_{min} and T at 92 km for the SSW 2009 is not related to the anticorrelation between temperature variations at different heights.

Siskind et al. [2017] have detected a significant increase in NO concentration and absorption of short radio waves in January 2008, as compared to January 2009, from 80 to 90 km. The authors attributed this difference to higher geomagnetic activity in 2008 and, as a result, more intense NO formation at high latitudes and its transfer to the mid-latitude mesosphere. Note that the increase in absorption (increase in f_{min}) in 2008 as compared to 2009 is also observed in our studies (see Figures 3 and 5). Thus, in 2009 f_{min} variations occur against a background of lower absorption than in 2008; it is obvious that the amplitude of f_{min} variations against lower absorption will be smaller. As mentioned above, f_{min} sets the critical absorption level at which the signal-to-noise ratio is sufficient to observe reflections from the ionosphere. Thus, f_{min} variations depend on variations not only in absorption, but also in noise level. With sufficiently large absorption variations, the noise contribution to f_{min} variations is negligible. As the range of absorption variations decreases, the noise contribution to f_{min} variations increases, which can lead to a significant decrease in the correlation between T and f_{min} variations, due to the fact that the latter are generally defined by noise level. As a result, the lack of correlation between the day-to-day variations in f_{min} and T at 92 km for the SSW 2009 may be related to low background absorption during the period of interest.

For the SSW 2013, the correlation between day-to-day variations in f_{min} and $T92$ is lower than for the SSW 2008. This decrease may be associated with the factors considered — significant changes in solar activity during the SSW 2013 and a lower correlation between temperature variations at different heights in 2013 than in 2008.

CONCLUSION

We have analyzed the responses of the minimum frequency of ionogram reflections f_{min} and the MLT temperature to the winter sudden stratospheric warmings in 2008, 2009, and 2013. Intense quasi-periodic variations in f_{min} running to 40 % in 2008 and 50 % in 2013 have been found.

The main result of the research is the detection of the high correlation between day-to-day variations in the minimum frequency of ionogram reflections and the atmospheric temperature at an altitude of 92 km for the SSW 2008 (R=0.89 for a 31-day interval approximately corresponding to the period between the first and last maximum of the mean zonal temperature at 10 hPa). The physical explanation for the high correlation is that a rise in temperature leads to an increase in both the electron density [Kazimirovsky et al., 2003; Schneider et al., 2025] and the electron-neutral collision frequency [Schneider et al., 2025; Schmitter, 2011], which increases absorption and f_{min}. A temperature drop leads to the opposite effect.

Another important result is that it is for the altitude of 92 km that the correlation between f_{min} and tempera-

ture is the highest. This result is consistent with the conclusions drawn in [Siskind et al., 2017], where through numerical simulation it was shown that the maximum differential absorption at a frequency of 5 MHz corresponds to the lower part of the E layer (about 95 km).

At the same time, the correlation analysis of day-to-day variations in f_{min} and $T92$, performed for other SSWs, has found three different cases: high correlation for the SSW 2008, no correlation for the SSW 2009, and moderate correlation for the SSW 2013. When interpreting the results, the main problem was to explain the lack of correlation for the SSW 2009. The following version is proposed: the lack of correlation for the SSW 2009 may be due to low background absorption during the period under study. In this case, the f_{min} variations may largely be determined by noise levels rather than by absorption. For the SSW 2013, the correlation between day-to-day variations in f_{min} and $T92$ was lower than for the SSW 2008. This decrease may be caused by significant changes in solar activity during the SSW 2013 and the lower correlation between temperature variations at different heights in 2013 than in 2008.

The results are important for estimating the increase in absorption of short radio waves during winter sudden stratospheric warmings.

The research was financially supported by the Russian Science Foundation (Project No. 25-17-00187 [https://rscf.ru/project/25-17-00187/]). The works on observations and data pre-processing were supported by the Ministry of Science and Higher Education of the Russian Federation. The results were partially obtained using the Core Shared Research Facility “Angara” of ISTP SB RAS [http://ckp-rf.ru/catalog/ckp/3056/] and the Large-Scale Research Facilities (LSRF) “Optical instruments”.

REFERENCES

Davies K. *Ionospheric Radio Waves.* Blaisdell Publishing Company, 1969, 460 p.

Goncharenko L., Chau J. L., Condor P., et al. Ionospheric effects of sudden stratospheric warming during moderate-to-high solar activity: Case study of January 2013. *Geophys. Res. Lett.* 2013, vol. 40, pp. 1–5. DOI: 10.1002/grl.50980.

Hoffmann P., Singer W., Keuer D. Variability of the mesospheric wind field at middle and Arctic latitudes in winter and its relation to stratospheric circulation disturbances. *J. Atmos. Solar-Terr. Phys.* 2002, vol. 64, pp. 1229–1240. DOI: 10.1016/S1364-6826(02)00071-8.

Hoffmann P., Singer W., Keuer D., Hocking W.K., Kunze M., Murayama Y. Latitudinal and longitudinal variability of mesospheric winds and temperatures during stratospheric warming events. *J. Atmos. Solar-Terr. Phys.* 2007, vol. 69, pp. 2355–2366. DOI: 10.1016/j.jastp.2007.06.010.

Kazimirovsky E., Herraiz M., De La Morena B.A. Effects on the ionosphere due to phenomena occurring below it. *Surv. Geophys.* 2003, vol. 24, pp. 139–184. DOI: 10.1023/A:1023206426746.

Klimenko M.V., Klimenko V.V., Koren’kov Y.N., et al. Modeling of response of the thermosphere-ionosphere system to sudden stratospheric warmings of years 2008 and 2009. *Cosmic Res.* 2013, vol. 51, iss. 1, pp. 54–63. DOI: 10.1134/S001095251301005X.

Limpasuvan V., Richter J.H., Orsolini Y.J., et al. The roles of planetary and gravity waves during a major stratospheric sudden warming as characterized in WACCM. *J. Atmos. Solar-Terr. Phys.* 2012, vol. 78–79, pp. 84–98. DOI: 10.1016/j.jastp.2011.03.004.

Lukianova R., Kozlovsky A., Shalimov S., et al. Thermal and dynamical perturbations in the winter polar mesosphere-lower thermosphere region associated with sudden stratospheric warmings under conditions of low solar activity. *J. Geophys. Res. Space Phys.* 2015, vol. 120, pp. 5226–5240. DOI: 10.1002/2015JA021269.

Manney G.L., Schwartz M.J., Krueger K., et al. Aura Microwave Limb Sounder observations of dynamics and transport during the record-breaking 2009 Arctic stratospheric major warming. *Geophys. Res. Lett.* 2009, vol. 36, L12815. DOI: 10.1029/2009GL038586.

Matsuno T. A dynamical model of the stratospheric sudden warming. *J. Atmos. Sci.* 1971, vol. 28, pp. 1479–1494. DOI: 10.1175/1520-0469(1971)028<1479:ADMOTS>2.0.CO;2.

Medvedeva I., Ratovsky K. Studying atmospheric and ionospheric variabilities from long-term spectrometric and radio sounding measurements. *J. Geophys. Res.: Space Phys.* 2015, vol. 120, iss. 6, pp. 5151–5159. DOI: 10.1002/2015JA021289.

Medvedeva I., Ratovsky K. Effects of the 2016 February minor sudden stratospheric warming on the MLT and ionosphere over Eastern Siberia. *J. Atmos. Solar-Terr. Phys*. 2018, vol. 180, pp. 116–125. DOI: 10.1016/j.jastp.2017.09.007.

Medvedeva I., Ratovsky K. Manifestation of wave activity in the upper atmosphere during winter sudden stratospheric warmings. *Modern Problems of Remote Sensing of the Earth from Space.* 2020, vol. 17, iss. 6, pp. 159–166. DOI: 10.21046/2070-7401-2020-17-6-159-166.

Medvedeva I.V., Semenov A.I., Pogoreltsev A.I., Tatarnikov A.V. Influence of sudden stratospheric warming on the mesosphere/lower thermosphere from the hydroxyl emission observations and numerical simulations. *J. Atmos. Solar-Terr. Phys.* 2019, vol. 187, pp. 22–32. DOI: 10.1016/j.jastp.2019.02.005.

Pancheva D., Mukhtarov P. Stratospheric warmings: The atmosphere-ionosphere coupling paradigm. *J. Atmos. Solar-Terr. Phys.* 2011, vol. 73, iss. 3, pp. 1697–1702. DOI: 10.1016/j.jastp.2011.03.006.

Pancheva D., Lastovicka J., de La Morena B.A. Quasi-periodic fluctuations in ionospheric absorption in relation to planetary activity in the stratosphere. *J. Atmos. Terr. Phys.* 1991, vol. 53, pp. 1151–1155. DOI: 10.1016/0021-9169(91)90065-F.

Perminov V.I., Pertsev N.N. The behavior of emissions and temperature of the mesopause during stratospheric warmings according to observations at midlatitudes. *Geomagnetism and Aeronomy.* 2013, vol. 53, iss. 6, pp. 780–784. DOI: 10.1134/S0016793213060108.

Polyakova A.S., Chernigovskaya M.A., Perevalova N.P. Ionospheric effects of sudden stratospheric warmings in Eastern Siberia region. *J. Atmos. Solar-Terr. Phys.* 2014, vol. 120, pp. 15–23. DOI: 10.1016/j.jastp.2014.08.011.

Schmitter E.D. Remote sensing planetary waves in the mid-latitude mesosphere using low frequency transmitter signals. *Ann. Geophys.* 2011, vol. 29, iss. 7, pp. 1287–1293. DOI: 10.5194/angeo-29-1287-2011.

Schneider H., Wendt V., Banyś D., et al. Impact of sudden stratospheric warming and elevated stratopause events on the very low frequency radio signal. *J. Geophys. Res.: Space Phys.* 2025, vol. 130, e2024JA033320. DOI: 10.1029/2024JA033320.

Shefov N.N. Relations between the hydroxyl emission of the upper atmosphere and the stratospheric warmings. *Gerlands Beitr. Geophysik.* 1973, vol. 82, iss. 2, pp. 111–114.

Shepherd M.G., Cho Y.M., Shepherd G.G., et al. Mesospheric temperature and atomic oxygen response during the January 2009 major stratospheric warming. *J. Geophys. Res.* 2010, vol. 115, A07318. DOI: 10.1029/2009JA015172.

Shpynev B., Kurkin V., Ratovsky K., et al. High-midlatitude ionosphere response to major stratospheric warming. *Earth, Planets and Space.* 2015, vol. 67, 18. DOI: 10.1186/s40623-015-0187-1.

Siskind D.E., Coy L., Espy P. Observations of stratospheric warmings and mesospheric coolings by the TIMED SABER instrument. *Geophys. Res. Lett.* 2005, vol. 32, L09804. DOI: 10.1029/2005GL022399.

Siskind D.E., Zawdie K., Sassi F., et al. Global modeling of the low and mid latitude ionospheric D and lower E regions and implications for HF radio wave absorption. *Space Weather*. 2017, vol. 15, pp. 115–130. DOI: 10.1002/2016SW001546.

Vargin P.N, Medvedeva I.V. Temperature and dynamical regimes of the Northern Hemisphere extratropical atmosphere during sudden stratospheric warming in winter 2012–2013. *Izvestiya, Atmospheric and Oceanic Physics.* 2015, vol. 51, iss. 1, pp. 12–29. DOI: 10.1134/S0001433814060176.

Walterscheid R.L., Sivjee G.G., Roble R.G. Mesospheric and lower thermospheric manifestations of a stratospheric warming event over Eureka, Canada (80 N). *Geophys. Res. Lett.* 2000, vol. 27, iss. 18, pp. 2897–2900. DOI: 10.1029/2000GL003768.

Yasyukevich A.S. Variations in ionospheric peak electron density during sudden stratospheric warmings in the Arctic region. *J. Geophys. Res. Space Phys.* 2018, vol. 123, pp. 3027–3038. DOI: 10.1002/2017JA024739.

Yasyukevich A.S., Chernigovskaya M.A., Shpynev B.G., Khabituev D.S., Yasyukevich Y.V. Features of winter stratosphere small-scale disturbance during sudden stratospheric warmings. *Remote Sens.* 2022, vol. 14, 2798. DOI: 10.3390/rs14122798.

Yigit E., Medvedev A.S. Internal wave coupling processes in Earth's atmosphere. *Adv. Space Res.* 2015, vol. 55, iss. 4, pp. 983–1003. DOI: 10.1016/j.asr.2014.11.020.

URL: http://disc.gsfc.nasa.gov/Aura (accessed July 15, 2025).

URL: http://gmao.gsfc.nasa.gov/research/merra/ (accessed July 15, 2025).

URL: https://rscf.ru/project/25-17-00187/ (accessed July 15, 2025).

URL: http://ckp-rf.ru/ckp/3056/ (accessed July 15, 2025).

Original Russian version: Ratovsky K.G., Medvedeva I.V., published in Solnechno-zemnaya fizika. 2026, vol. 12, no. 1, pp. 45–54. DOI: 10.12737/szf-121202606.

How to cite this article

Ratovsky K.G., Medvedeva I.V. Comparative analysis of responses of minimum frequency of ionogram reflections and mesosphere-lower thermosphere temperature to winter sudden stratospheric warmings. *Sol.-Terr. Phys*. 2026, vol. 12, iss. 1, pp. 40–49. DOI: 10.12737/stp-121202606.